LAWRENCE
LIVERMORE
NATIONAL
LABORATORY

UCRL-JRNL-225345

Substrate Creep on The Fatigue Life of A Model Dental Multilayer Structure

J.K. Zhou, M. Huang, X. Niu, W. soboyejo

October 17, 2006

Journal of Biomedical Materials Research

Substrate Creep on The Fatigue Life of A Model Dental Multilayer Structure

J. Zhou[+], M. Huang[×], X. Niu[*] and W.O. Soboyejo[*]

[+]Lawrence Livermore National Laboratory, Livermore, CA 94551

[×]Silicon Technology Development, Texas Instruments Incorporated, Dallas, TX 75243

[*]Princeton Institute for the Science and Technology of Materials and

Department of Mechanical and Aerospace Engineering

Princeton University, Princeton, NJ 08544

Abstract: In this paper, we investigated the effects of substrate creep on the fatigue behavior of a model dental multilayer structure, in which a top glass layer was bonded to a polycarbonate substrate through a dental adhesive. The top glass layers were ground using 120 grit or 600 grit sand papers before bonding to create different sub-surface crack sizes and morphologies. The multilayer structures were tested under cyclic Hertzian contact loading to study crack growth and obtain fatigue life curves. The experiment results showed that the fatigue lives of the multilayer structures were impaired by increasing crack sizes in the sub-surfaces. They were also significantly reduced by the substrate creep when tested at relatively low load levels i.e. $P_m < 60$ *N* (P_m is the maximum magnitude of cyclic load). But at relatively high load levels i.e. $P_m > 65$ *N*, slow crack growth (SCG) was the major failure mechanisms. A modeling study was then carried out to explore the possible failure mechanisms over a range of load levels. It is found that fatigue life at relatively low load levels can be better estimated by considering the substrate creep effect (SCE).

Keywords: Hertzian contact, dental materials, adhesive resin, polycarbonate, creep, fatigue, slow crack growth.

INTRODUCTION

In a variety of dental restoratives, a ceramic top layer is bonded to dentin or dentin-like substrate using adhesive resin to produce a multi-layer structure (Figure 1a) [1-4], in which the hard ceramic layer on top provides mechanical and chemical protection for the compliant substrate below. When concentrated loads are applied, the sub-surface region of the top ceramic layer is subjected to significant tensile stress [5-7]. Consequently, cracks in the sub-surface are prone to grow, leading ultimately to total degeneration.

The effect of pre-existing cracks on the strength of the top ceramic layer has been the subject of numerous studies [7-11] where a flat sandwich model (FSM) structure consisting of a top ceramic layer, an adhesive joint layer, and a polymeric substrate was tested under Hertzian contact loading (Figure 1b). Transparent top glass layers elastically equivalent to the enamel or crowns in actual dental restoratives were often used to facilitate in situ observation of crack growth. In order to induce radial crack growth in the sub-surface of the top ceramic layers, initial cracks were produced using various methods including sandblasts [7-9], random grinding with silicon carbide sandpapers [9,10], and micro-indention [11]. These studies showed that the sub-surface cracks caused significant mechanical degradation under cyclic or monotonic loading [7-11].

It is found that the creep of the polymeric substrate had significant effects on the strength of the top ceramic layer [6,12,13]. When the loading rates increased from 1 N/s to 1000 N/s, the strength of the ceramic layer doubled [13]. Such creep effects were found in FSM structures with different combinations of top and substrate materials, such as glass on polycarbonate [6,14], glass on Z100 restorative [6,13], silicon on polycarbonate [14], and ceramic on Z100 restorative [6,13].

Until now, substrate creep effects on fatigue behavior (tested on FSM structures) have not been studied. In this study, a glass-adhesive-polycarbonate FSM was used to investigate the substrate creep effects on fatigue behavior under cyclic contact loading. Elastically equivalent soda-lime glass slides were used as top layers to facilitate the monitoring of crack growth. The top glass layers were processed into two sets of specimens with different sub-surface crack sizes ground with silicon carbide sand papers of 120 grit or 600 grit before bonding. It has been found that fatigue life tested at relatively high load levels, i.e. $P_m > 65\ N$ (P_m is the maximum

magnitude of cyclic load) can be well predicted by the slow crack growth (SCG) model. But the fatigue life corresponding to relatively low load levels, i.e. $P_m < 60\ N$, is merely a fraction of the SCG model prediction. We believed that the significant discrepancy is due to the substrate creep. A modeling framework involving substrate creep can provide a better estimate for fatigue life.

MATERIALS AND EXPERIMENTAL METHODS

Microscope soda-lime glass slides (EMS, Halfield, PA) with dimensions of 25.4 mm (L) × 25.4 mm (L) × 1 mm (H) were used as top layers. They were ground using 120 grit or 600 grit silicon carbide sand papers (Buehler, Lake Bluff, IL) before bonding to create different sub-surface crack sizes and morphologies. After grinding, the glass slides were sonicated in deionized water for 30 min and then in acetone for 10 min. Isopropanol was then applied to the rough surfaces prior to blowing them with high pressure nitrogen gas. The surface morphologies and crack sizes were examined using a surface profiler (KLA-Tencor, San Jose, CA). A 5 μN load was used to enable the profiler tip to explore cracks of different sizes ranging from nanoscale to microscale.

Polycarbonate plates (Lexan, National City, CA) with dimensions of 25.4 mm (L) x 25.4 mm (W) x 12.8 mm (H) were used as the substrates. An FSM structure was created by bonding the prepared glass slide to the polycarbonate plate using 3M RelyXTEM adhesive (3M ESPE, St Paul, MN), and light cured for 40 seconds. In the FSM structure, the ground glass surface became sub-surface when bonded to the polycarbonate substrate, as shown schematically in Figure 1b. The mechanical properties of these materials are summarized in Table 1 [6,15].

Cyclic Hertzian contact testing was carried out in a desktop servo-hydraulic Instron 8872 testing machine (Instron, Canton, MA) equipped with a 500 N load cell. A sinusoidal cyclic load was applied through a WC ball with a diameter of 3.18 mm (Figure 1b). The load frequency, *f*, was 5 Hz. A Questar® telescope (New Hope, PA) was set up and focused on the sub-surface regions right beneath the contact area. The crack growth and pop-in were recorded using Pinnacle Studio 9.0 (Pinnacle, Elgin, IL) software that was installed in a computer connected to the Questar® telescope. The imaging rate was 15 frames per second, sufficient to capture crack growth and subsequent pop-in. The images were post-analyzed to obtain crack growth rate.

RESULTS

Sub-surface cracks

Figure 2a shows a three-dimensional sub-surface morphology of a top glass layer that was ground with 120 grit sand papers. Parallel cracks were generated varying in length in a range from less than 100 μm to about 1 millimeter. Their depths also vary. A distribution of the crack depths in a representative region of about 1×1 mm^2 is shown in Figure 2b. The average crack depth is about 1.5 μm. 90% are less than 4.0 μm deep. The deepest cracks are about 16 μm deep. The positive values in the horizontal axis in Figure 2b suggest that there are protrusions in the glass substrate. They may be silicon carbide particles remaining in the glass surface.

The morphology and depth distribution of the cracks generated using 600 grit sand papers were similar to those made using 120 grit papers, with the exception of shallower cracks, shown in Figure 3. A long crack about 1 μm deep, the maximum depth found in this glass slide, was observed in the scanned area of 500×500 μm^2. The average crack depth was only ~200 nm, which is one order smaller than those obtained using 120 grit sand papers (Figure 2). The average and maximum values of the sub-surface cracks of the two sets of specimens are summarized in Table 2.

In the cyclic testing, efforts were made to set up the WC ball above one of the biggest sub-surface cracks visible in the telescope, as schematically shown in Figure 1b.

Crack growth and S-N curves

Figure 4 shows crack growth in the sub-surface of a FSM specimen prepared using 600grit sand papers. It was tested with a maximum load of 45 N. Figure 4a was taken before applying the load. The white spots, indicated by white arrows, are the sub-surface cracks. Another crack, invisible in Figure 4a, started growing after applying cyclic loads. The location of this crack is indicated by a circle. Figure 4b shows the crack after ~ 997 cycles of testing. Significant crack growth was observed in the next ~ 9, 900 cycles, with increasing growth rates (Figure 4c). The crack then "popped in" at ~ 10,010 cycles, leading ultimately to failure of the top glass layer (Figure 4d). The cracks in Figure 4b and 4c appear distant from the immediate contact area. This is due to the orientation of the cracks. If a crack in the region right under the contact area is not exactly parallel to the optical axis of the telescope, the light is reflected in an

inclined angle with respect to the optical axis of the telescope. Crack images taken under these conditions are not indicative of their exact locations.

Sub-surface crack sizes and the corresponding cycles were obtained by carefully analyzing the in situ images recorded during testing. Representative curves showing crack size versus cycles are presented in Figures 5a and 5b for the two sets of specimens. For the first set of specimens with top glass layers prepared using 600 grit sand papers, the crack growth behavior was dependent on the applied maximum load levels. When the maximum load levels were relatively low, i.e. $P_m < 60\ N$, most of the specimens exhibited four crack growth stages. The first stage was a short startup stage in which a crack grew and became rapidly visible. This was followed by a slow growing stage, in which the crack grew slowly. Figure 4b shows a crack at the end of this stage. The third was a fast growing stage. The cracks grew significantly with increasing rates in this stage, and their sizes doubled (Figure 4c). In the final stage, the cracks "popped-in" to maximum size within decades of cycles. The four stages of crack growth are illustrated schematically in Figure 6. In contrast, cracks grew rapidly under high maximum load levels, i.e. $P_m > 65\ N$, and "popped in" to maximum size, leading ultimately to the failure of the top glass layer.

The second set of specimens, whose sub-surfaces were prepared using 120 grit sand papers exhibited similar crack growth behavior (Figure 5b). At relatively low load levels, i.e. $P_m < 60\ N$, the cracks underwent four stages of growth. Cracks grew rapidly and resulted in the failure of the top glass layer when the loads were relatively high, i.e. $P_m > 65\ N$. The number of cycles corresponding to the onset of crack pop-in was accordingly defined as the fatigue life of the specimen (Figure 6).

Cyclic contact load testing was carried out on multiple specimens using different maximum load levels, and the maximum load levels versus the numbers of cycles until failure were obtained for both sets of specimens. The results are plotted in Figures 7a and 7b. As expected, the deeper surface cracks resulted in shorter fatigue lives for specimens that were tested at relatively high load levels, i.e. $P_m > 65\ N$. This is consistent with previous studies [7,11,19]. The difference diminishes at relatively lower load levels, i.e. $P_m < 60\ N$.

SLOW CRACK GROWTH

According to slow crack growth (SCG) theory [16,17], the relationship between the maximum load, P_m, and the fracture time, t_f, is given [14, 19]:

$$P_m^{\,N} t_f = 2AN^{0.47} \tag{1}$$

where $N = 18$ is crack velocity exponent [17], and A is a fitting parameter which is independent of load and time [19]. The fracture time, t_f, is determined by loading frequency, f, and the number of cycles to failure, n, i.e. $t_f = n/f$. Rewriting Equation 1 in a log-log format gives:

$$\log P_m = -\frac{1}{N}\log n + \log(2AfN^{0.47})^{1/N} \tag{2}$$

When all other quantities are constants, the log-log plot of P_m versus the number of cycles to failure is linear. Fitting curves from Equation 2 are superimposed in Figures 7a and 7b, and designated as predictions of slow crack growth (SCG) model. At relatively high load levels, i.e. $P_m > 65\ N$, the experimental data are consistent with the model prediction. However, at lower load levels, i.e. $P_m < 60\ N$, the measured data are significantly lower than the SCG model prediction. This suggests that slow crack growth is not the only mechanism of fatigue failure at relatively low load levels.

SUBSTRATE CREEP EFFECTS

Recent studies have shown that creep of polymeric substrates has significant effects on deformation of glass-cement-polymer FSM structures [6,12,13]. As a result of the substrate (actually a combination of adhesive resin and polycarbonate substrate) creep, tensile stresses in the sub-surface regions increase with time, leading to reduced fatigue life compared to the predictions of SCG model (Equation 2). The time required for a radial crack to fracture a specimen can be obtained by the following equation [12, appendix A]:

$$\int_0^{t_f} \sigma^N dt = D \tag{3}$$

where, $D \approx \frac{K_{IC}^N}{(N/2-1)v_0\psi^N a_i^{N/2-1}}$, is independent of load and time, a_i is the initial crack depth, v_0 is crack velocity coefficient, ψ is a crack geometry coefficient, which is 1.12 for an edge crack, σ is the stress in the sub-surface of the top glass layer, K_{IC} is the fracture toughness of soda-lime glass, which is in a range between 0.6 and 0.8 MPa√m [20]. In this study, we take 0.7 for the calculation. During fatigue testing, the stress will be assumed to vary sinusoidally between 0 and maximum stress amplitude, $\sigma_{\max}$, that is:

$$\sigma = \frac{\sigma_{\max}}{2}\left[1+\sin\left(2\pi ft - \frac{\pi}{2}\right)\right] \tag{4}$$

Note that the maximum stress is not a constant due to substrate creep, i,e, $\sigma_{\max} = \sigma_{\max}(t)$.

Substituting Equation 4 into Equation 3 gives:

$$\int_0^{t_f}\left(\frac{\sigma_{\max}(t)}{2}\right)^N\left[1+\sin\left(2\pi ft - \frac{\pi}{2}\right)\right]^N dt = D \tag{5}$$

It is difficult to obtain an explicit solution from the integration of Equation 5. Hence, we consider a simple worst-case scenario, in which the stress is taken to be the maximum value, $\sigma_m = \sigma_{\max}(t_f)$. Under this simplicity and for periodic loading, we can solve Equation 5 by multiplying the number of cycles to failure with the integration over one cycle. We notice that $\int_0^1\left[1+\sin(2\pi x - \pi/2)\right]^N dx = 2^{N-1}/N^{0.47}$ [19], and take the maximum stress in the sub-surface of the top glass layer as $P_m = \frac{B\sigma_m d^2}{\log(CE_c/E_s)}$ [21]. The relationship between the maximum load and the failure time is:

$$P_m{}^N\left\{\log\left[\frac{CE_c}{E_s(t_f)}\right]\right\}^N t_f = 2DN^{0.47}B^N d^{2N} \tag{6}$$

where d is the thickness of top glass layer, E_c and E_s are Young's moduli of the top layer and substrate, respectively, and B and C are dimensionless coefficients. The quantity C is expected to be close to 1, because the tensile stress concentrate in the top coating must vanish when $E_c = E_s$ [19]. For simplicity, C is taken to be 1 in this paper. Also, B was estimated to be 1.455 by fitting with the finite element simulations of bi-layer model [12]. As the substrate creeps, the

Young's modulus, E_s, varies with time. Here, we model the substrate as a 3-parameter spring-dashpot solid model (Zener model) as shown in Figure 8. The Young's modulus is then given by:

$$\frac{1}{E_s} = \frac{1}{k_1}\left\{1 - \frac{k_2}{k_1 + k_2}\exp\left[-\frac{k_1 k_2 t}{\eta(k_1 + k_2)}\right]\right\} \tag{7}$$

where t is the time, k_1, k_2 and η are the parameters used in the viscoelastic model (Figure 8). These parameters were measured using creep testing and listed in Ref. [6]. Substituting Equation 7 into Equation 6 gives the relation between the maximum load and the elapsed time for the sub-surface radial crack to fracture the top glass layer as:

$$P_m{}^N\left[\log\left(\frac{CE_c}{k_1}\left\{1 - \frac{k_2}{k_1 + k_2}\exp\left[-\frac{k_1 k_2 t_f}{\eta(k_1 + k_2)}\right]\right\}\right)\right]^N t_f = H \tag{8}$$

where $H = \frac{2\mathrm{N}^{0.47} B^N d^{2N} K_{IC}^N}{(N/2-1)\nu_0 \psi^N a_i^{N/2-1}}$, independent of load and time. Equation 8 gives the relation between the maximum load, Pm, and the time to induce the failure, t_f. If the foundation is elastic, that is $\eta \approx \infty$, Equation 8 reduces to Equation 1 and $A = \frac{B^N d^{2N} K_{IC}^N}{(N/2-1)\nu_0 \psi^N a_i^{N/2-1} \log(CE_c / E_s)}$. To compare the predictions of the slow crack growth (SCG) model (Equation 1) and the substrate creep effects (SCE) model (Equation 8) with the experimental results, we take $N = 18$, $\nu_0 = 1.6 m/\mu s$, which were measured from the experimental data published in Ref. (17), $K_{IC} = 0.7 MPa\sqrt{m}$ for glass, and $d = 1mm$ for our specimens. Figure 7 clearly shows that the SCE model, which considers the substrate creep behavior, gives much better estimates for fatigue life than SCG model. Since the viscoelastic parameters change with time, the fitting curves obtained using Equation 8 are not smooth [6].

The initial crack depth, a_i, is the only fitting parameter. The fitting values are 1.6 μm for the 600 grit sand paper case and 2.5 μm for the 120 grit sand paper case, respectively. These initial crack sizes do not perfectly match the measured values as listed in Table 2, particularly for the 120 grit sand paper case. Several factors could cause the discrepancy. First of all, perfect materials are assumed in the model, as contrast to the real tested samples with defects and

inevitable structural variations. Secondly, the accurate crack depth under the ball is difficult to determine. Thirdly, the crack to induce failure may not be the one under the contact points between the loading ball and the top glass surface. Finally, the crack geometry in the subsurface could also affect model estimations. Nevertheless, this is a first piece of work to study the substrate creep effects. It is yet to be perfect, but a good point to start with. More vigorous work is clearly needed in the future.

DISCUSSION

Comparing the two sets of data in Figure 7, one can see that the fatigue lives of the top glass layers were significantly reduced by the deep cracks produced using coarser sand papers (120 grit versus 600 grit). The FSM structure prepared using untreated glass slides did not fail at load levels less than 90 N (Figures 7a and 7b). When the applied loads were greater than 100 N, they failed due to top cone crack growth under monotonic loading. This observation implies that the substrate creep interacts with pre-existing sub-surface cracks to reduce fatigue life.

At relatively high load levels, i.e. $P_m > 65\ N$, the FSM structures failed within a limited number of cycles (a few minutes). Within such a short duration the contribution from substrate creep to overall deformation was not substantial. However, when the FSM structures were tested at relatively lower load levels, i.e. $P_m < 60\ N$, it took a longer time to fracture the top glass layer, possibly a few hours. For specimens prepared using 600 grit sand papers the fatigue life corresponding to a load level of 50 N was close to 10000 cycles, only a fraction of the life predicted by the SCG model. In both cases, the crack size was relatively small (less than ~ 100 μm) before the last crack "pop-in" stage, in which crack grew to a size about 800 μm within decades of cycle. Compared to the overall fatigue life, this is a small fraction. In this sense, the small crack growth (SCG) theory and the substrate creep effect (SCE) models can be used to model the crack growth behavior. Furthermore, the SCG model predictions agree with the experimental data, suggesting that the use of SCG model and SCE model is suitable, and the relevant parameters in these two models are valid. Therefore, we believe that slow crack growth is the primary failure mechanism, and substrate creep accelerates crack growth, leading to premature fatigue failure of the top glass layer when the applied load levels were relatively low.

In this study, the cracks in the sub-surface of the top glass layers were produced by grinding the glass slides on sand papers along a fixed direction. The sub-surface cracks generated using this methods have large length-to-depth ratio, and they are parallel to each other, as shown in Figures 2a and 3a. Such crack geometry is significantly different from a typical surface crack that is randomly oriented and has a comparable crack length and depth. This could possibly lead to different crack growth behavior in the multilayer structure. The effect of the crack geometry on fatigue failure of dental restorative may be investigated in the future studies.

It is well known that initial crack size has significant effects on the fatigue life of multilayer dental structure [2,8,15,17-19]. To examine the fatigue life dependence on the initial crack size, the predictions by both SCG and SCE models are presented in Figure 9 for a series of initial crack sizes. It shows that the initial crack sizes do not affect the shape of the prediction curves. But increasing crack size significantly reduces the fatigue life. These are true for both models. This is consistent with the results of our earlier studies [6,12,13]. Corresponding to these initial crack sizes, the H and A values are also calculated and listed in Table 3. The parameter A and H are two parameters that are independent on load and time, but dependent on initial crack size. The values of H and A decrease with increasing initial crack sizes.

It is important to note here that the cyclic contact loading applied during occlusal contact was not continuous. A certain amount of recovery time is implied because contact loads are not continuously applied directly to teeth. Such recovery can reduce the long-term effects of substrate creep, especially when compared to the current results obtained from specimens that were loaded continuously until failure. Further work is needed to explore the extent to which substrate creep/recovery effects contribute to the fatigue life under actual occlusal contact.

SUMMARY AND CONCLUSIVE REMARKS

This study explores the effects of the substrate creep on the fatigue behavior of a dental multilayer structure. A summary of the work is provided below, along with salient conclusions.

1. Glass slides were ground using 120 grit or 600 grit sand papers before bonding to prepare two sets of FSM specimens with different sub-surface crack sizes. When tested at relatively

high load levels, i.e. $P_m > 65\ N$, the fatigue lives of both sets of specimens were well predicted by the SCG model (Equation 2). The deeper sub-surface cracks significantly impaired the fatigue life.

2. When tested at relatively lower load levels, i.e. $P_m < 60\ N$, the sub-surface cracks below the contact areas underwent four-stage growth: start-up stage, slow crack growth stage, fast crack growth stage, and crack pop-in stage. The fatigue life is only a fraction of the predictions made by SCG model.
3. The substantial discrepancy between the measured fatigue life and SCG prediction can be attributed to the substrate creep, which results in increasing magnitudes of crack opening stresses in the sub-surface. This accelerates crack growth, and the fatigue life can be better estimated by the SCE model (Equation 8).
4. The current study suggests that substrate creep should be considered when the mechanical performance of dental restorative is evaluated. However, such effects may also be relaxed when the occlusal loads are removed. Further work is needed to establish the significance of substrate creep during normal occlusal conditions in which contact loads may be removed for significant durations.

ACKNOWLEDGEMENTS

The research was supported by the National Institutes of Health (Grant No. P01 DE10956). The authors are grateful to the Program Manager, Dr. Eleni Kouslevari, for her encouragement and support. The authors would also like to thank Prof. Dianne Rekow and Prof. Van Thompson of New York University for useful technical discussions. JKZ appreciate supports from Dr. L.L. Hsiung. Part of the work was performed under the auspices of the U. S. Department of Energy by the University of California, Lawrence Livermore National Laboratory under Contract No. W-7405-Eng-48.

Appendix A - Slow Crack Growth under Varying Stress Condition

If a crack with an initial size, a_i, is in the sub-surface of the top glass layer (Figure 1b), it will slowly grow due to tensile stress, σ, induced by Hertzian contact loading. The growth rate is governed by the stress intensity factor, K, as [17]:

$$da/dt = v_0 (K/K_{IC})^N \tag{A1}$$

where a is crack size, K_{IC} is fracture toughness of glass, and N and v_0 are, respectively, crack velocity exponent and coefficient. The stress intensity factor, K, is expressed as:

$$K = \psi \sigma a^{1/2} \tag{A2}$$

where ψ is a crack geometry coefficient, which is 1.12 for edge crack. Combining Equations (A1) and (A2), and integrating to the time at fracture, t_f, gives:

$$\int_0^{t_f} \sigma^N dt = D. \tag{A3}$$

where $D = \dfrac{K_{IC}^N \left(a_i^{1-N/2} - a_f^{1-N/2}\right)}{(N/2-1) v_0 \psi^N}$, a_i and a_f are the initial and final crack sizes, respectively. Since $a_f >> a_i$, D can be simplified as $\dfrac{K_{IC}^N}{(N/2-1) v_0 \psi^N a_i^{N/2-1}}$, which is independent of load and time.

References:

1. http://www.animated-teeth.com

2. Kelly JR. Ceramics in restorative and prosthetic dentistry. *Annual Review of Material Science* 1997; 27: 443-468.

3. Willems, G., Lambrechts, P., Braem, M., Celis, J.P., and Vanherle, G. A classification of dental composites according to their morphological and mechanical characteristics. *Dental Materials* 1992; 8:310-319, 1992.

4. Kelly JR. Clinically relevant approach to failure testing of all-ceramic restorations. *The Journal of Prosthetic Dentistry* 1999; 81: 652-661.

5. Shrotriya P, Wang R, Katsube N, Seghi R and Soboyejo WO. Contact damage in model dental multilayers: an investigation of the influence of indenter size. *Journal of Materials Science: Materials in Medicine* 2003; 14:17-26.

6. Huang M, Niu X, Shrotriya P, Rekow ED, Thompson VP and Soboyejo WO. Contact damage of dental multilayers: viscous deformation and fatigue mechanisms. *Journal of Engineering Materials and Technology* 2005; 127: 33-39

7. Zhang Y, Lawn BR, Rekow ED, Thompson VP. Effect of sandblasting on the long-term strength of dental ceramics. *Journal of Biomedical Materials Research A* 2004; 71B: 381-386.

8. Kosmac T, Oblak C, Jevnikar P, Funduk N, Marion L. The effect of surface grinding and sandblasting on flexural strength and reliability of Y-TZP zirconia ceramic. *Dental Materials* 1999; 15: 426-433.

9. Kosmac T, Oblak C, Jevnikar P, Funduk N, Marion L. Strength and reliability of surface treated Y-TZP dental ceramics. *Journal of Biomedical Materials Research A* 2000; 53: 304-313.

10. Miranda P, Pajares A, Guiberteau F, Cumbrera FL, Lawn BR Role of flaw statistics in contact fracture of brittle coatings. *Acta Materialia* 2001; 49 (18): 3719-3726.

11. Zhang Y, Lawn BR. Fatigue sensitivity of Y-TZP to microscale sharp-contact flaws. *Journal of Biomedical Materials Research A* 2000; 72B (2): 388-392.

12. Huang M, Niu X and Soboyejo WO. Creep induced rate effects on radial cracks in multilayerd structures, *Journal of Materials Science: Materials in Medicine* (in press).

13. Niu X and Soboyejo WO. Effects of loading rate on the deformation and crack of dental multilayers: experiments and models (*Submitted for publication*).

14. Lee CS, Kim DK, Sanchez J, Miranda P, Pajares A, Lawn BR. Rate effects in critical loads for radial cracking in ceramic coatings. *Journal of American Ceramic Society* 2002; 85 (8): 2019-2024.

15. Zhou J, Huang M, Sagnang F and Soboyejo WO. Interfacial Failure of A Dental Cement Composite Bonded to Glass Substrates. *Dental Materials (*in press).

16. Wiederhorn, S.M. and Bolz, L.H., 1970. Stress corrosion and static fatigue of glass, *Journal of American Ceramic Society* 53(10), 543-548.

17. Wiederhorn, S.M., 1974. Subcritical crack growth in ceramics. In: *Fracture Mechanics of Ceramics*, vol. 2. Edited by Bradt, R.C., Lange, F.F., and Hasselman, D.P.H., Plenum, New York.

18. Lawn BR, Pajares A, Zhang Y, Deng Y, Polack MA, Lloyd IK, Rekow ED and Thompson VP. Materials design in the performance of all-ceramic crowns. *Biomaterials* 2004; 25: 2885–2892.

19. Kim DK, Jung YG, Peterson IM and Lawn, BR. Cyclic fatigue of intrinsically brittle ceramics in contact with spheres. *Acta Materialia* 1999; 47 (18): 4711-4725.

20. Callister WD, Jr. Materials Science and Engineering, 3rd Edition. New York, Wiley, 2003.

21. Kim HW, Deng Y, Miranda P, Pajares A, Kim DK, Kim HE, Lawn BR. Effect of flaw state on the strength of brittle coatings on soft substrates. *Journal of American Ceramic Society* 2001; 84 (10): 2377-2384.

List of Tables

List of Figures

Figure 8: 3-parameter spring-dashpot solid model (Zener model).

Figure 9: The effects of initial crack size and substrate creep on the fatigue life of the multilayer structure.

Table 1: Material properties used in calculation.

Materials	E (GPa)	Poisson's ratio
Glass	70	0.2
Adhesive resin	3.2	0.4
Polycarbonate	2.3	0.4

Table 2: Surface crack depths generated using 120 grit or 600 grit sand papers.

	Average depth (μm)	Maximum depth (μm)
120 grit	1.5	16.0
600 grit	0.2	1.0

Table 3: Values of H and A corresponding to various sizes of initial cracks.

Initial crack size (μm)	H (N^{18})	A (N^{18})
0.5	2.77E+43	2.40E+42
1.0	1.08E+41	9.36E+39
1.6	3.00E+39	2.60E+38
2.5	7.00E+37	6.07E+36
5.0	2.77E+35	2.40E+34
15.0	4.22E+31	3.66E+30

Figure 1: (a) Schematic illustration of a dental restoration structure consisting of a top ceramic layer, an adhesive bond layer and dentin. (b) A flat sandwich model (FSM) structure consisting of a top ceramic layer, an adhesive joint layer and a polymeric substrate.

(a)

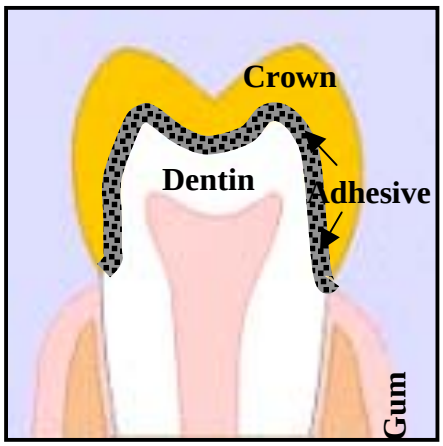

(b)

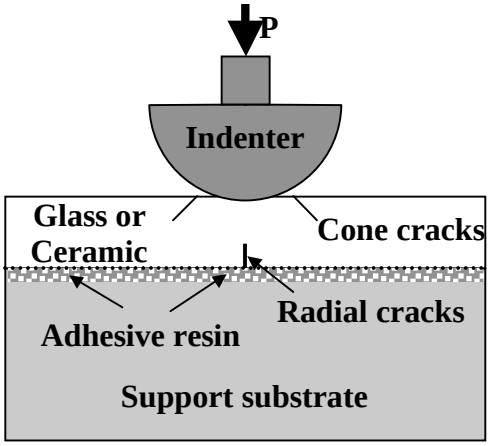

Figure 2: The glass sub-surface cracks and morphology prepared using 120 grit sand papers: (a) 3-D surface morphology; (b) crack depth distribution in a representative area of ~1 mm × 1 mm.

(a)

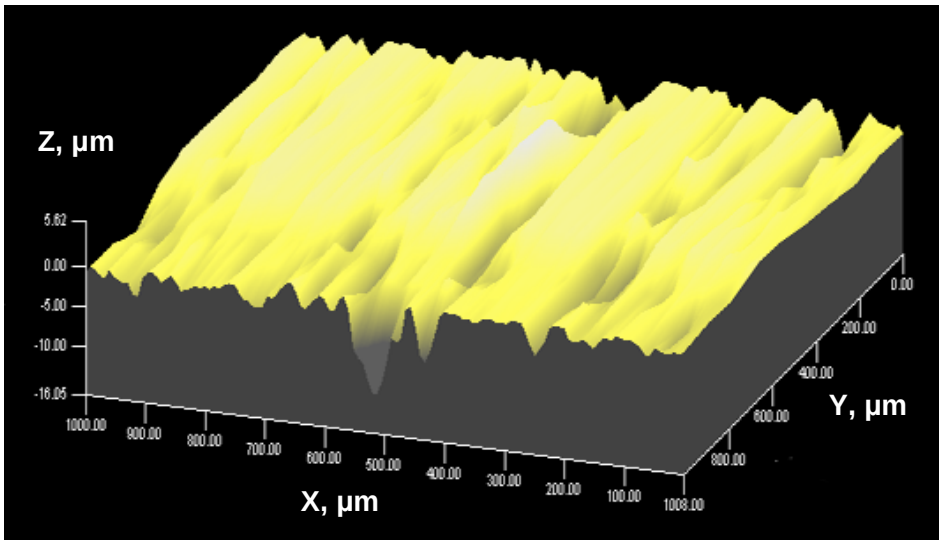

(b)

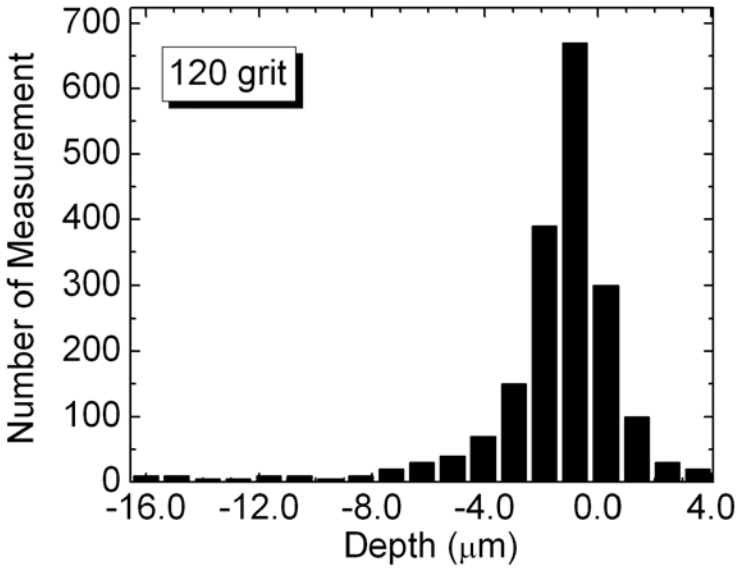

Figure 3: The glass sub-surface cracks and morphology prepared using 600 grit sand papers: (a) 3-D surface morphology; (b) crack depth distribution in a representative area of ~ 500 μm × 500 μm.

(a)

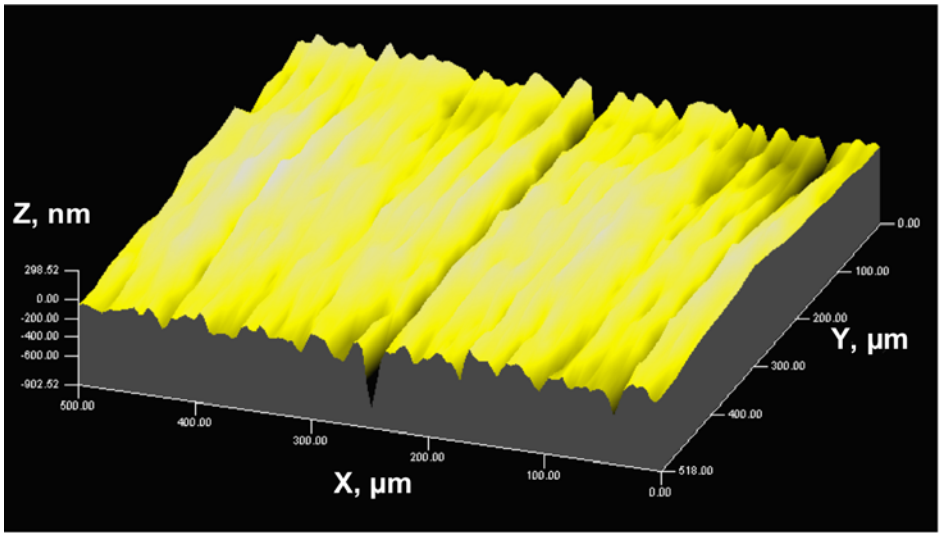

(b)

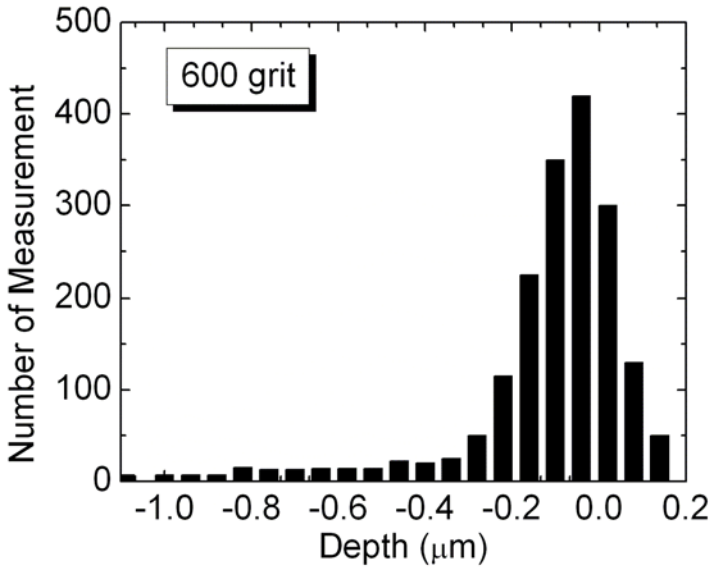

Figure 4: Crack growth and pop-in corresponding to increasing number of contact fatigue cycles: (a) n = 0, (b) n = 997, (c) n = 9,989, and (d) n = 10,010. Scale bars are 500 μm. The specimen was prepared using 600 grit sand papers, and tested at $P_m = 45\ N$.

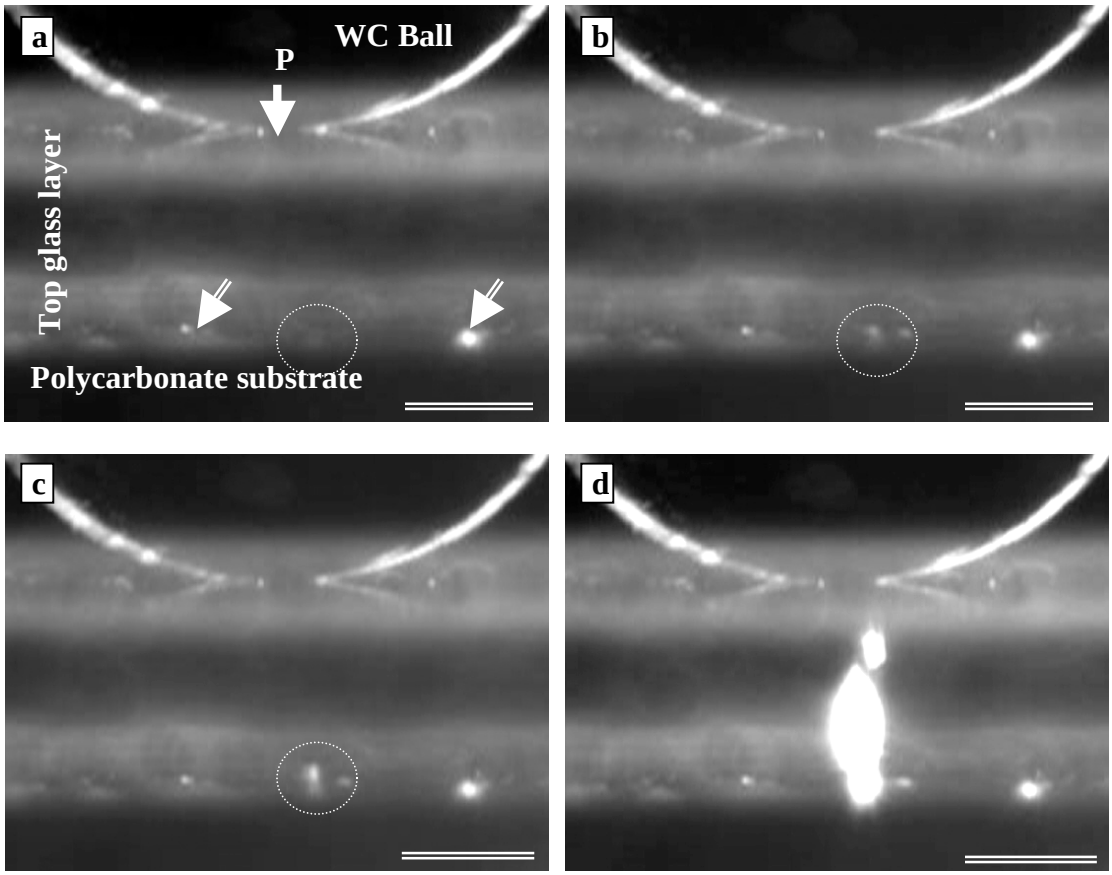

Figure 5: Representative plots of crack size versus number of cycles for (a) specimens prepared using 600 grit sand papers; and (b) specimens prepared using 120 grit sand papers.

(a)

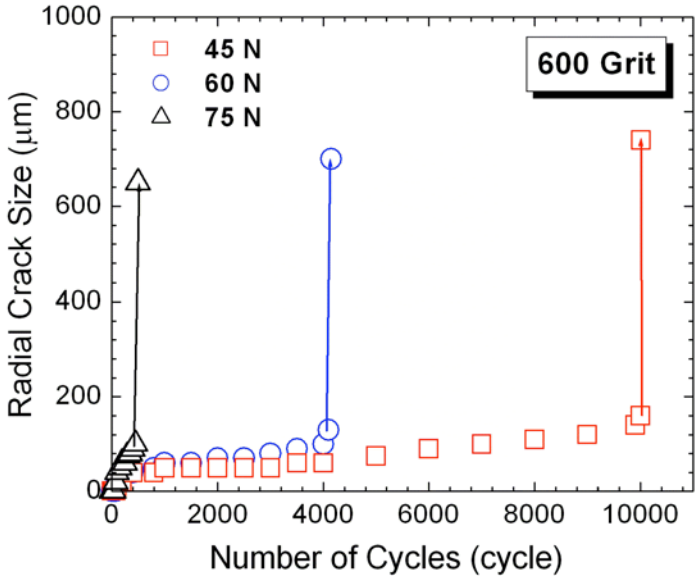

(b)

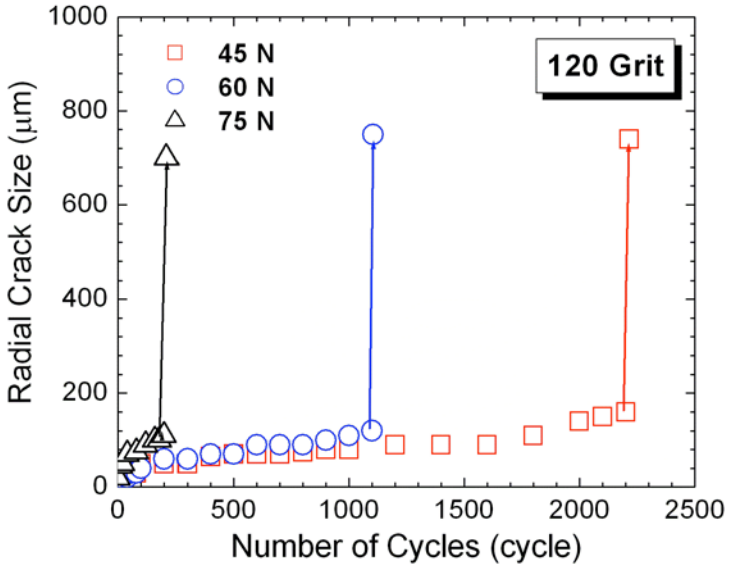

Figure 6: Schematic illustration of the sub-surface crack growth behavior at relatively low load levels, i.e. $P_m < 60\ N$.

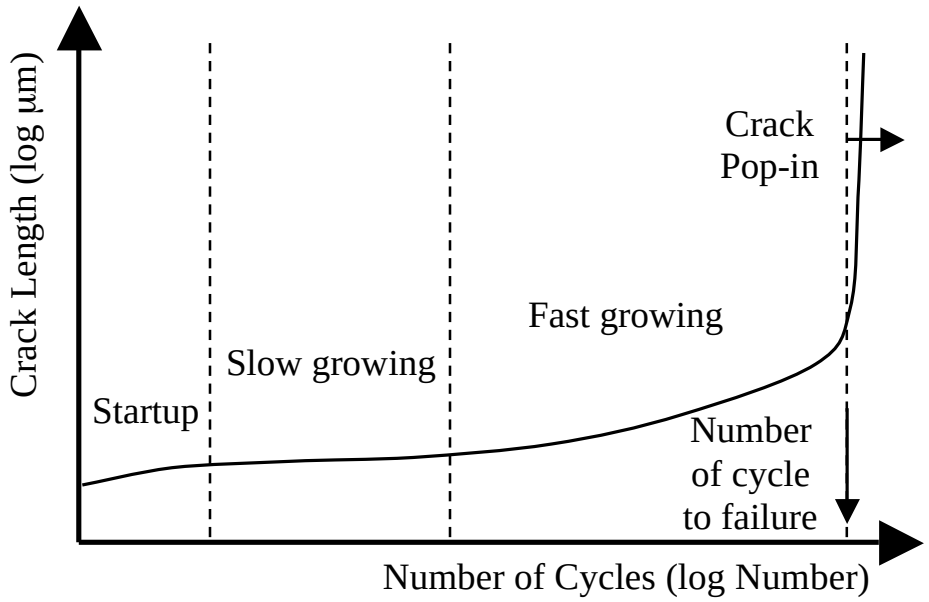

Figure 7: Measured fatigue life curves for specimens with different crack sizes in sub-surfaces prepared using (a) 600 grit sand papers and (b) 120 grit sand papers. The SCG model and SCE model predictions are also plotted for comparison.

(a)

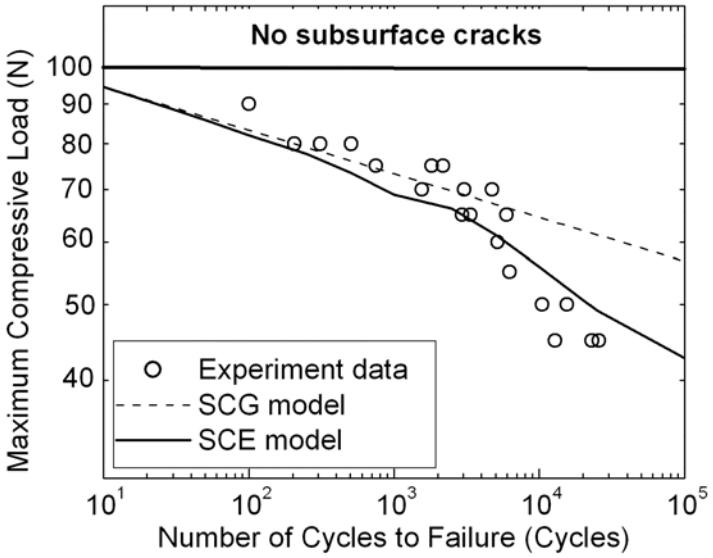

(b)

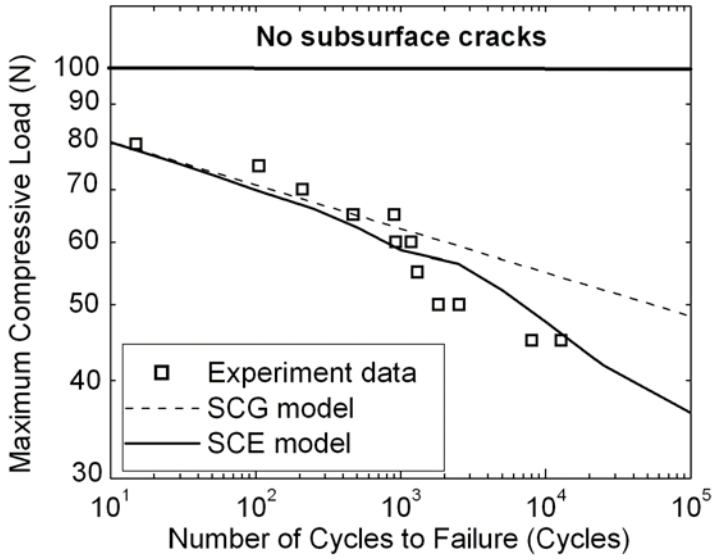

Figure 8: 3-parameter spring-dashpot solid model (Zener model).

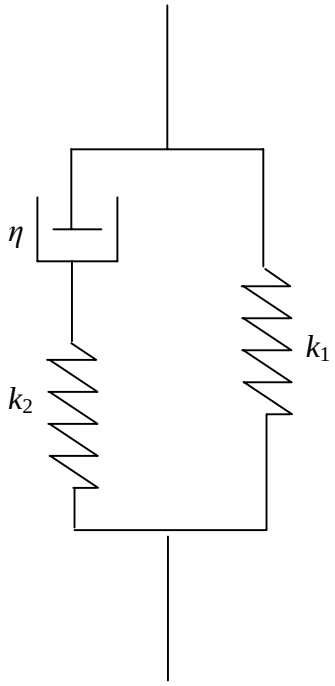

Figure 9: Effects of initial crack size on the fatigue life of the multilayer structure.